Third International Conference on Sustainable Construction Materials and Technologies http://www.claisse.info/Proceedings.htm

Behavior of cement treated sand under large deformations

Kh. Adeel Tariq [1] and Takeshi Maki [2]

[1]Ph.D. Student, Department of Civil and Environmental Engineering, Saitama University, Saitama, Japan, khawajaadeel@hotmail.com
[2]Associate Professor, Department of Civil and Environmental Engineering, Saitama University, Saitama, Japan, maki@mail.saitama-u.ac.jp
[1]Saitama University, 255 Shimo-o-kubo, Sakura ku, Saitama shi, Saitama 338-8570, Japan
[2]Saitama University, 255 Shimo-o-kubo, Sakura ku, Saitama shi, Saitama 338-8570, Japan

ABSTRACT

Mixing of sand with cement is one of the fastest growing techniques in many coastal and offshore areas and is becoming means of improving poor soil conditions. The purpose of this study is to understand the behavior of cement treated sand under large deformation. Cylindrical specimens were casted by using cement (high early strength), sand (S) and limestone powder (L) for water to cement ratio (W/C) of 100, 130, 150, 170 and 190 % and their softening behavior is investigated under cyclic compressive stress. In order to measure the internal strain distribution of cement treated sand, specially made silicone bar is used. The influences of material strength and height to diameter ratio (H/D) on compression fracture zone length and fracture energy are investigated. Relationships between compression fracture zone length, fracture energy and compressive stress are suggested.

Keywords: Cement, Sand, Limestone powder, Fracture zone length, Fracture energy,

INTRODUCTION

Soil improvement is referred to as a procedure in which addition of some special soil or chemical material improves properties of the natural soil. The engineering behavior of soil depends on the particle size distribution and the composition of the particles. It is possible to significantly change the property of given soil by removing some selected fractions of the soil. Generally the cost of addition/removal technique of stabilization can be low as compared with other techniques of soil improvement. The construction procedure, cost and results obtained from addition/removal stabilization technique depends mostly on the type of problem and nature of soil at field condition.

The method of improvement necessarily depends on the character of the soil and its deficiencies. In general it is required to improve the strength of the in situ soil. Type of stabilizer depends on the treated soil, for example for sandy soils cement is preferred and for clayey soils lime is preferred to be used as a stabilizer because of its mineral composition. Compressibility problems of weak soil can be reduced by using consolidation, by filling the voids with an appropriate material or cementing the grains with a rigid material. Ground improvement by cement mixing have been applied extensively for structure foundation, excavation control and liquefaction mitigation.

Soil cementation can be found naturally, or induced artificially for the purpose of improving the bearing capacity of weak soils. Cementation plays a significant role in the engineering behavior of soils, and has been investigated by engineers around the world (Ali et al., 1997). The mechanical properties of most cement stabilized soils change over time, therefore the time-related performance of such treated soils is essential in understanding their durability and long-term effectiveness (Probaha et al., 2000). Cement content does increase the peak strength of the treated soil, it also increases the stiffness thereby reducing the strain at which failure occurs (Lee et al., 2002). Cement bentonite containment barriers appear to offer a cost-effective solution to the problems of contaminated land. There have been no reports of failures of such barriers and as such their use has increased particularly to contain contaminated sites (Stephen et al., 1999).

The viscosity of cement-based material can be improved by decreasing the water/cementitious material ratio or using a viscosity-enhancing agent. It can also be improved by increasing the cohesiveness of the paste through the addition of filler, such as limestone powder. The use of limestone powder improves the properties of fresh and hardened concrete such as workability and durability (Zhou et al., 2010). For a fixed water content, high powder volume increases interparticle friction due to solid–solid contact. This may affect the ability of the mixture to deform under its own weight and pass through obstacles (Nawa et al., 1998).

When concrete fails, damage usually concentrates in a localized region in the structure. The localization behavior can influence the structural behavior, especially the post-peak behavior. Strain softening of concrete occurs when microcracks which begin before the peak strength coincides to form a zone of damage (Figure 1a), weakening the concrete, so its load carrying capacity starts diminished, which ultimately leads to complete collapse. Additional deformation of zone of damage weakens the specimen further and continued softening occurs. When specimen is short, damage appears to be concentrated in entire length of the specimen. Fracture behavior of cement treated sand is not clarified so far. The fracture zone and the localization behavior of cement treated sand have to be clarified for accurate understanding of the structural behavior up to the failure.

In the softening region, the damaged or failure zone continues to strain while the undamaged zone elastically unloads. In the compression, damage zone or failure zone model proposed by Markeset and Hillerborg, the softening behavior in the damaged zone is due to a combination of longitudinal tensile cracking and the formation of a localized inclined shear band (Markeset et al., 1995). In the uniaxial case, localization initiates at the peak stress. The relationship between compression fracture zone length (L_p) and compression fracture energy with compressive strength of concrete is as follows (Nakamura et al., 1999):

$$G_{fc} = 8.8\sqrt{f_c} \tag{1}$$

$$L_p = \frac{1300}{\sqrt{f_c}} \tag{2}$$

Soft/weak soils are complex, rate-dependent non-linear multi-phase materials, and major advances have been made in recent years in advanced constitutive modeling of such materials. Mixing of sand with cement is one of the possible ways to improve the foundation conditions especially for sandy soils. This technique is gaining popularity these days because it is relatively easy to use. However, long term behavior of cement treated sand has not yet been clarified.

Specimen geometry and boundary conditions will also affect the strain softening behavior because they affect the size and shape of failure zone relative to overall specimen; investigating these influences is beyond the scope of experimental work presented here. This paper describes the mechanical behavior of cement treated sand, determination of compression fracture zone length and compression fracture energy of cement treated sands. The energy absorbed per unit of area within compression fracture zone is the Compression fracture energy, G_{fc} (Figure 1b).

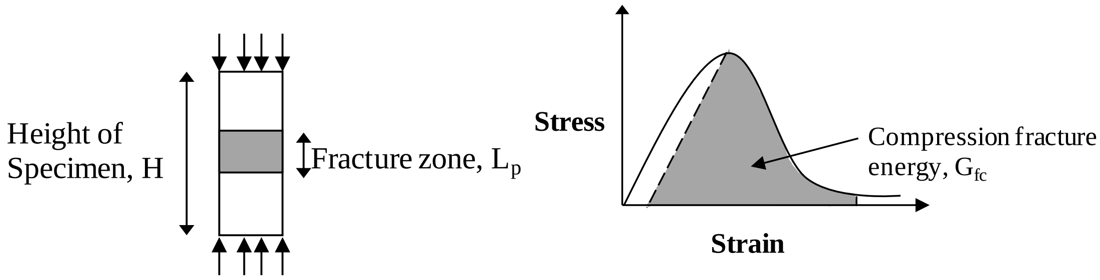

(a) (b)

Figure 1. (a) Compression fracture zone length (b) Compression fracture energy explanation

EXPERIMENTAL APPARATUS AND PROCEDURE

High early strength cement, limestone powder and sand were used to make the test specimens. Poorly graded sand (uniformly-graded) passing 5mm sieve was used having coefficient of uniformity and curvature about 2.2 and 1.0 respectively which was calculated according to Unified soil classification system (ASTM D2487, 2006). The water absorption of sand was 1.32%. The density of sand, cement and limestone powder was 2.63, 2.70 and 3.16 g/cm^3 respectively. Sand was first mixed with limestone powder; then with cement and finally water was added to the mix. Limestone powder was used to increase the viscosity of the paste and to make the mix more workable. The moisture which was already present in the limestone powder was ignored in the mix design.

The size of the test specimens are shown in Figure 2. Test variables were W/C = 100%, 130%, 150%, 170%, 190 %, C/S = 30%, and L/C = 130% by weight. These ratios were selected after trial experiments. W/C was varied in order to study the failure mechanism of high strength and relatively weaker cement treated sand. Unconfined compression tests were performed for curing period of 7 and 14 days. Curing is done by covering the specimens with wet clothes. The density of specimens was about 2100 kg/m^3.

In order to investigate the internal behavior of cement treated sand, strain gauges were attached to a specially made silicone bars which was placed at the center of the specimens and were kept straight with the help of wires of strain gauges (Figure 3). Silicone has very less stiffness (Young's Modulus about 0.4 GPa) as compared with cement treated sands, so it has less effect on strain gauges attached to it. The experiments were carried out under controlled loading conditions and the total average strain was measured externally by using transducers which were set between loading plates.

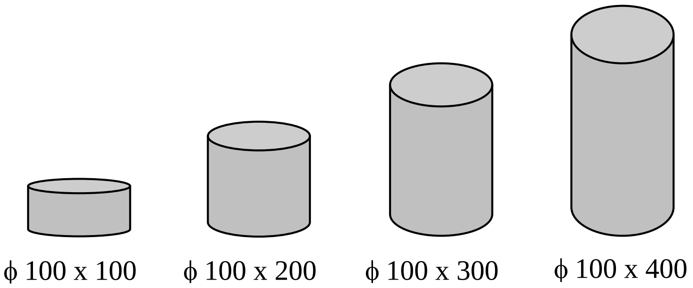

Figure 2. Size of test specimens (mm)

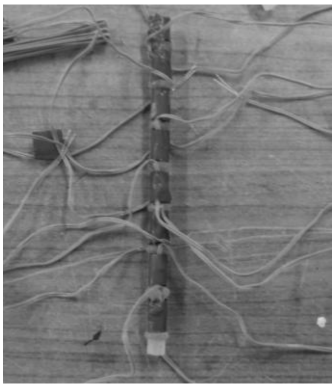

Figure 3. Strain gauges attached to silicone bar

TEST RESULTS AND DISCUSSION

Uniaxial compression test

The unconfined compression test was performed on test specimens in accordance with ASTM C39 (2005). Though, cement treated sand can bear compressive load but due to its plastic nature it undergoes volume change while performing compression test. Therefore, area correction is applied while calculating compressive strength of such cement treated sands. Corrected area, A is given as:

$$A = \frac{A_o}{(1-\varepsilon)} \tag{3}$$

A_o is initial average cross-sectional area, ε is average axial strain for given axial load (expressed as decimal) and it is calculated as:

$$\varepsilon = \frac{\Delta H}{H_o} \tag{4}$$

H_o is initial height of test specimen and ΔH is change in height of specimen.

Development of strength of specimens with curing times in terms of different W/C ratio is shown in Figure 4. It can be seen from the results that the maximum compressive stress (strength) is independent of the size of the test specimens for cement treated sands. Strain corresponding to peak stress (14days) for such cement treated sands was about 0.003 (Figure 5a).Young's modulus for 14 days curing period using W/C = 100 % was about 6 GPa (Figure 5b).

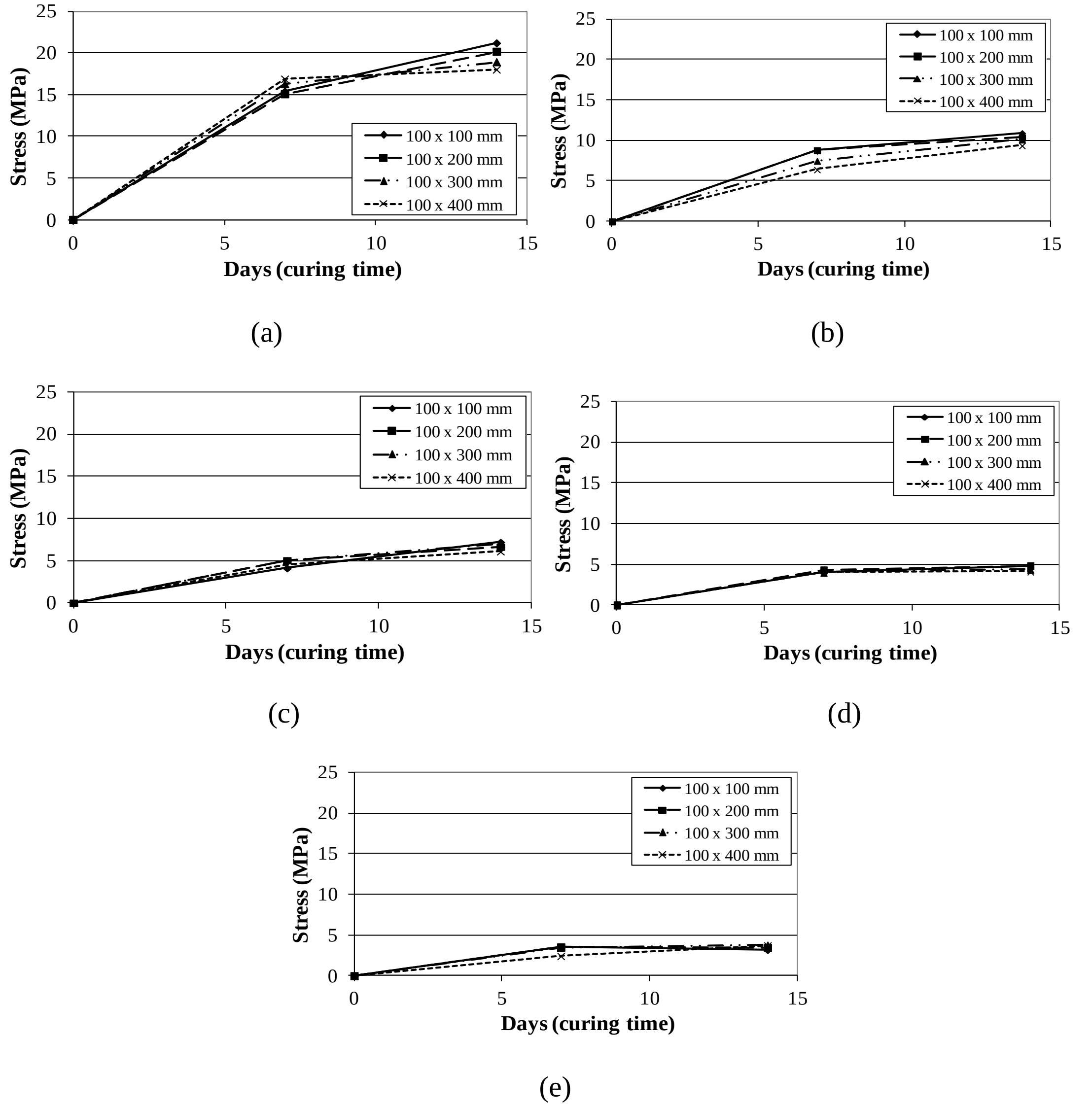

Figure 4. Comparison of maximum compressive stress for W/C = (a) 100% (b) 130% (c) 150% (d) 170% (e) 190%

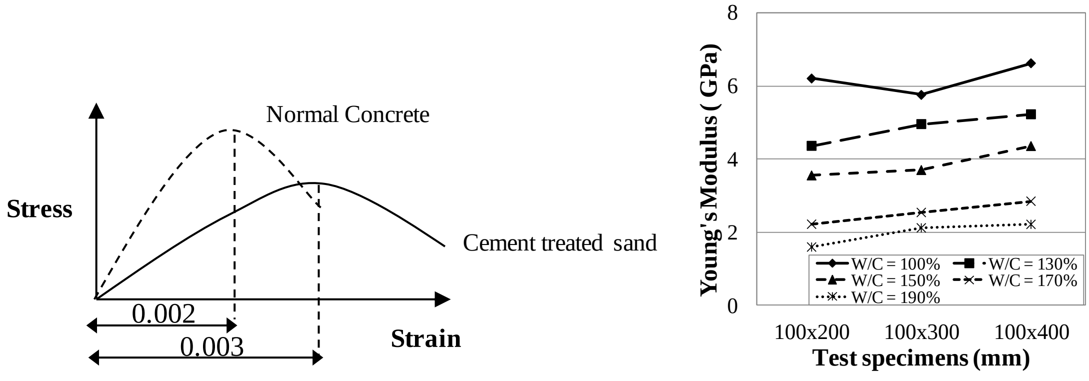

(a) (b)

Figure 5. (a) Schematic stress strain curve showing peak strain (b) Young's Modulus for different W/C ratios

Compression fracture zone length (L_p) and Compression fracture energy G_{fc}

Cyclic compression test was performed and results for 100 x 400 mm specimen (W/C = 100%) is shown in Figure 6a. Numbers in circle are indicating the loading cycle number. Strain distribution internally was measured by the strain gauges attached to silicone bar which was placed at the center of the test specimen (Figure 6b).

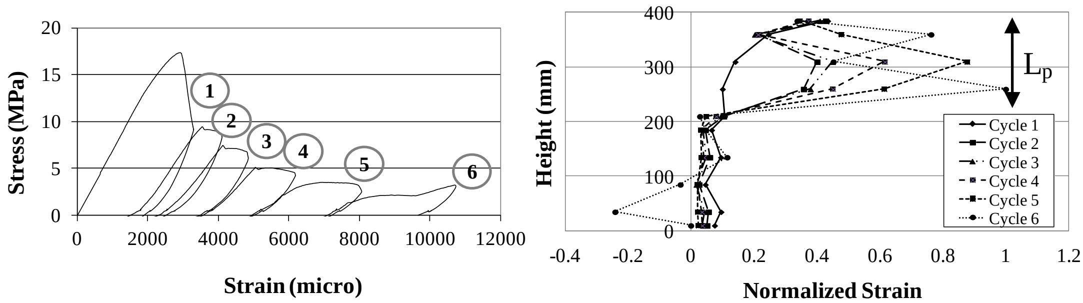

Figure 6. (a) Uniaxial cyclic load test on a 100 x 400 mm specimen of W/C = 100% (b) Internal strain distribution of a 100 x 400 mm specimen

The techniques to measure the compression fracture zone length directly for concrete are suggested by Nakamura et al. (1999) and later by Lertsrisakulrat et al. (2001). In this study the comparison of both techniques were carried out and suitable procedure for cement treated sand is suggested. According to Nakamura et al., compression fracture zone length can be defined as the increasing zone of the local strain from the test results.

However, Lertsrisakulrat et al. (2001), suggested determination of compression fracture zone length based on the quantification of energy absorbed throughout the specimen height and compressive fracture zone is defined as the zone in which the value of A_{inti} is larger than 15 percent of A_{int}. Where A_{inti} is the energy absorbed in each portion of the specimen and A_{int} is total energy absorbed throughout the specimen. Strain distribution for each loading cycle is shown in 6(b). Based on the concept of Nakamura et al. (1999), compression fracture zone length of this specimen is about 200 mm as failure zone can be identified from higher strain zone.

Local stress strain curve measured from inside the specimen for W/C = 100 % (100 x 400mm) specimen is shown in Figure 7a. It can be seen from local stress strain curve that some part shows increasing trend of strain (softening behavior) whereas some parts shows unloading behavior which distinguishes between failure zone and unloading part. Figure 7c shows the failed specimen. It can be seen from this figure that it is difficult to identify the failure zone from outside of the specimen.

The method suggested by Lertsrisakulrat et al. (2001), seems not feasible for cement treated sand or weaker material as the failure zone may consist of small fracture energy. Figure 8, shows energy consumed throughout the height of 100 x 400 mm (W/C = 100%) specimen calculated from local strain distribution. By using the method suggested by Lertsrisakulrat et al. (2001), compression fracture zone length comes out to be about 155 mm which is smaller than the actual compression fracture zone length measures from the local strain distribution which is about 200 mm. However, if compressive fracture zone is defined as the zone in which the value of $A_{int\,i}$ is larger than 5 percent of A_{int} then the failure zone can be identified correctly as shown in Figure 8.

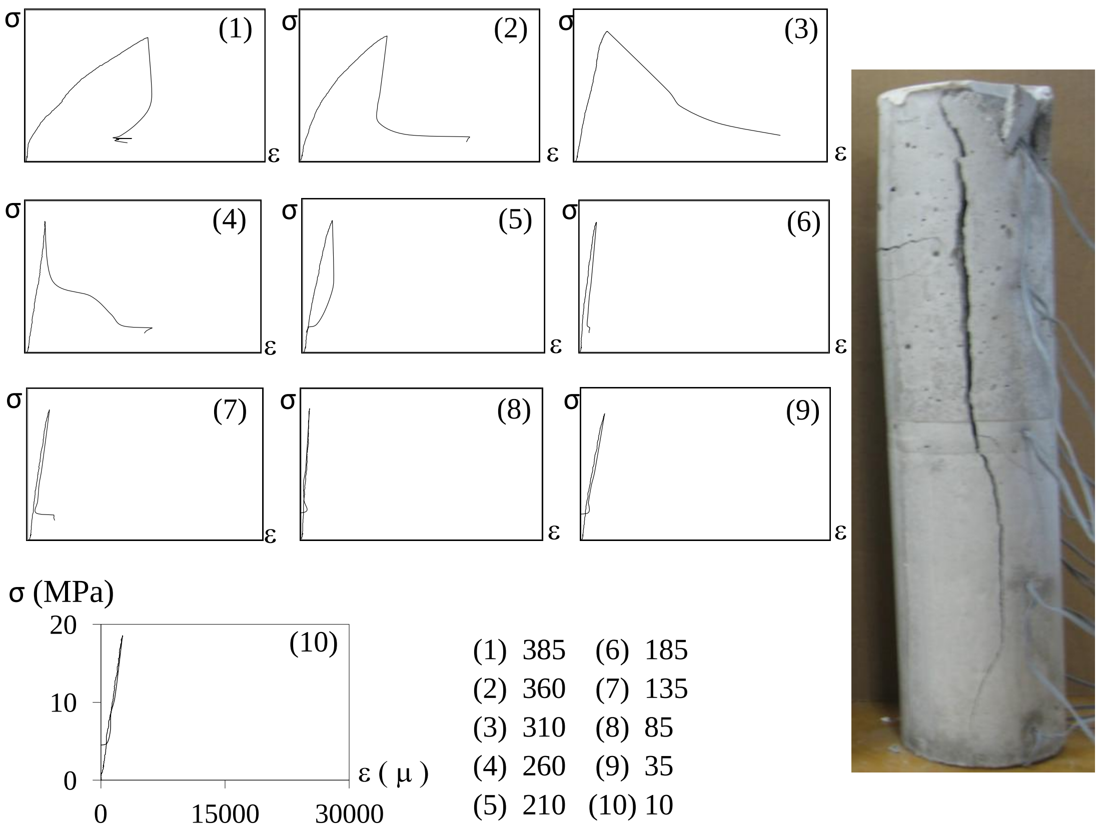

(a) Local Stress Strain curve (b) Stain gauge No. and located height (mm) (c) Failed specimen 100 x 400 (W/C = 100%)

Figure 7. Distinction between failure and unloading part

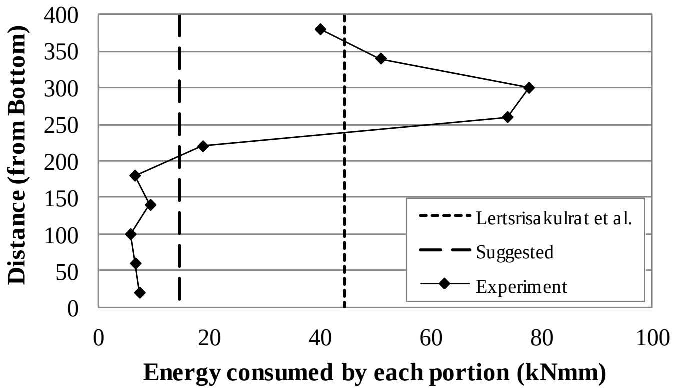

Figure 8. Evaluation of Compression fracture zone length based on local energy concept

Effect on compression fracture zone length with different H/D ratio is shown in Figure 9a. It can be seen that compression fracture zone length increases with the height until it reaches to a constant value of about 250 mm. Based on the test results (Figure 9b) following equation is proposed for the estimation of compression fracture zone length of cement treated sand from compressive strength:

$$L_p = \frac{600}{\sqrt{f_c}} \tag{5}$$

In conclusion of test results of different height specimens, it is found that strain localization only occurs in those specimens having height more than $L_{p.}$

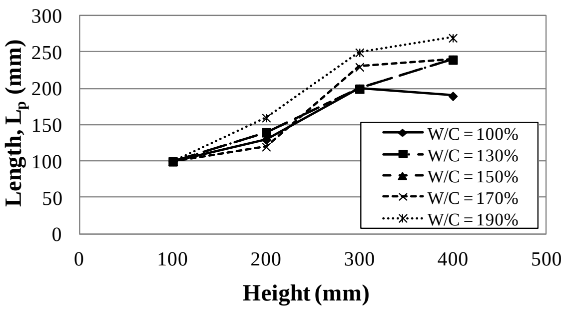

(a)

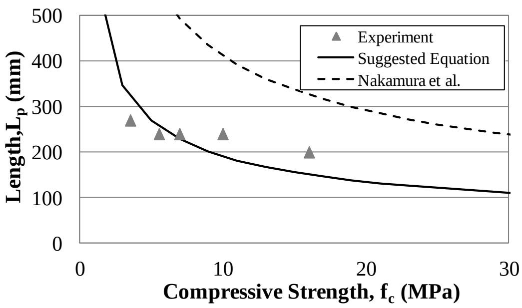

(b)

Figure 9. Compression fracture zone length variation with (a) height (b) compressive strength

Figure 10a, shows the results of compressive fracture energy. It can be seen that for H/D = 1, G_{fc}/f_c is slightly higher as compared with other H/D ratios. This may be due to problems which occurred during experiments like friction between loading plates etc, as smaller size specimen are relatively more sensitive to such conditions. It is shown that G_{fc}/f_c is a constant value regardless of H/D of the specimens for a particular W/C ratio of cement treated sand.

Based on the test results (Figure 10b) following equation is proposed for the estimation of compression fracture energy of cement treated sand from compressive strength:

$$G_{fc} = 3\sqrt{f_c} \tag{6}$$

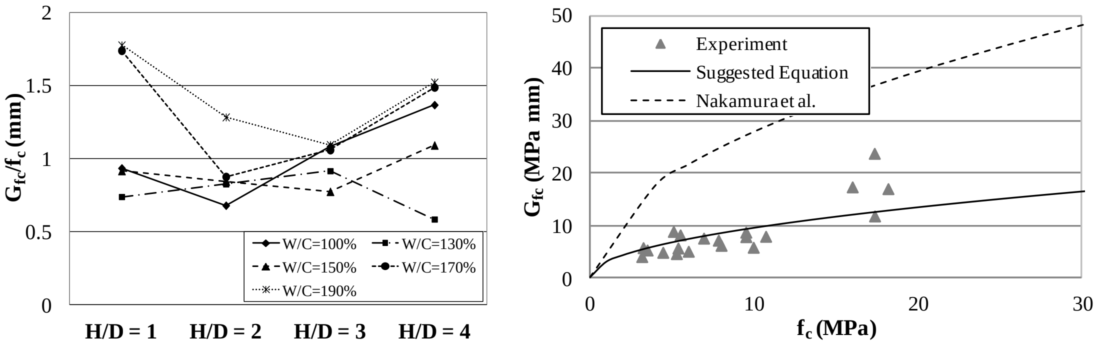

(a) (b)

Figure 10. Variation in compression fracture energy with (a) H/D ratio (b) Compressive stress

CONCLUSIONS

A series of uniaxial cyclic compression tests were carried out in order to investigate the fracture behavior of cement treated sand. Based on the test results, following are the conclusions:

1. Uniaxial compression tests were performed for specimens by varying H/D ratio from 1 to 4. Test results have indicated that maximum compressive stress of cement treated sand is independent of the size of the test specimen.
2. Compression fracture zone length extends throughout the height of specimens having H/D ratio less than or equal to one. Strain localization only occurs in those specimens having height more than L_p.
3. The test results show that the compression zone length increases with the height of the specimen and then it becomes constant to a height of about 250 mm.
4. Compression fracture energy of cement treated sand is a constant value independent of different H/D ratios.
5. Suggested relationship between compression fracture zone length, compressive fracture energy and compressive strength will be helpful in analyzing the behavior of cement treated sands.

REFERENCES

Ali, A.A. and Panos, D. K. (1997). “Behavior of Cemented sands-I. Testing.” *Int. J for Numerical and Analytical methods in Geomechanics*. 21, 533-547.

ASTM (American society for testing and materials) C39 (2005). “Standard test method for compressive strength of cylindrical concrete specimens.”

ASTM (American society for testing and materials) D2487 (2006). "Standard Practice for Classification of Soils for Engineering Purposes." (Unified Soil Classification System).

Lee, K. H. and Lee, S. (2002). "Mechanical properties of weakly bonded cement stabilized kaolin." *KSCE Journal of Civil Engineering*, Vol 6, No 4.

Lertsrisakulrat, T., Watanabe K., Matsuo, M., and Niwa, J. (2001). "Experimental study on parameters in localization of concrete subjected to compression". *JSCE Journal of Materials, Concrete, Structures and Pavements*, Vol 50, pp 309-321.

Markeset, G. and Hillerborg, A. (1995). "Softening of concrete in compression – localization and size effects"., *Cement and concrete research*, Vol 25, No 4, pp 702-708.

Nakamura, H. and Higai, T. (1999). "Compression fracture energy and fracture zone length of concrete"., JCI-C51E Seminar on Post peak behavior of reinforced concrete structures subjected to seismic loads- Recent advances and challenges on analysis and design, Vol 2, pp 259-272.

Nawa, T., Izumi, T., and Edamatsu, Y. (1998). "State-of-the-art report on materials and design of self-compacting concrete"., *Proc. of the Int. Workshop on Self-Compacting Concrete*, Kochi, Japan, 160–190.

Porbaha, A., Shibuya, S. and Kishida, T. (2000). "State of the art in deep soil mixing technology. Part III: Geomaterial characterization"., *Journal of Ground Improvement*, 3, pp.91–110.

Stephen, L., Garvin. and Carolyn, S.H. (1999). "The chemical compatibility of cement bentonite cut-off wall material." *Construction and Building Materials*. 13, 329-341.

Zhou, J., Qian, S., Beltran, S,G., Ye, G., Breugel, V,K. and Li, V. (2010). "Development of engineered cementitious composites with limestone powder and blast furnace slag"., *Material and Structures*, 43, pp. 803-814.